

## Research Article

# Adaptive Radio Frequency Interference Mitigation for Passive Bistatic Radar Using OFDM Waveform

Zhixin Zhao, Sihang Zhu, Yuhao Wang, Siyuan Cheng, and Sheng Hong

*School of Information Engineering, Nanchang University, Jiangxi 330031, China*

Correspondence should be addressed to Zhixin Zhao; zhaozhixin@ncu.edu.cn

Received 10 March 2016; Revised 30 June 2016; Accepted 25 July 2016

Academic Editor: Lorenzo Crocco

Copyright © 2016 Zhixin Zhao et al. This is an open access article distributed under the Creative Commons Attribution License, which permits unrestricted use, distribution, and reproduction in any medium, provided the original work is properly cited.

High frequency passive bistatic radar (HFPBR) is a novel and promising technique in development. DRM broadcast exploiting orthogonal frequency division multiplexing (OFDM) technique supplies a good choice for the illuminator of HFPBR. HFPBR works in crowded short wave band. It faces severe radio frequency interference (RFI) problem. In this paper, a theoretical analysis of the range-domain correlation of RFI in OFDM-based HF radar is presented. A RFI mitigation method in the range domain is introduced. After the direct-path wave rejection, the interference subspace is constructed using the echo signals at the reserved range bins. Then RFI in the effective range bins is mitigated by the subspace projection, using the correlation among different range bins. The introduced algorithm is easy to perform in practice and the RFI mitigation performance is evaluated using the experimental data of DRM-based HFPBR.

## 1. Introduction

HF passive bistatic radars (HFPBR) are a subset of bistatic radars exploiting noncooperative HF transmitters of opportunity. They have gained more and more attention in detecting low-flying and ocean ship targets as well as some remote sensing applications, for their advantages of both PBR (including having lower cost, being harder to detect, and being capable of directly and naturally facing the spectral compatibility issue) and HF over-the-horizon radars [1]. Digital broadcast is taking the place of traditional analog broadcast. With the trend of this, much research and development have been invested in PBR exploiting digital broadcast transmitters as a surveillance sensor in recent years [1–5]. DRM broadcast exploiting orthogonal frequency division multiplexing (OFDM) is accepted as the only standard for HF band by ITU-R, which has got rapid development globally, especially in Europe, in past years [6–8]. The use of OFDM signal provides frequency diversity to the system [9, 10]. DRM broadcast transmitter supplies good choices for the illuminator of HFPBR system, owing to its good signal properties and excellent low-altitude coverage.

RFI is introduced in HF radar since the frequency band 3–30 MHz is shared by many radio services. It is also

inevitable for HFPBR because DRM broadcasts have to share the usage of the current equipment and frequency bands of the analog transmission systems over a period of time called transition period. In HFPBR, surveillance and reference channels are needed to receive echoes of interest and reference signal, respectively. RFI will raise up the noise floor of the range-Doppler (RD) plot after the two-dimensional cross-correlation function (2D-CCF) when appearing in the surveillance channel. When the RFI to target echo ratio increases, target's peak-to-noise-floor ratio will decrease or the target would be masked completely [11]. Thus, RFI will lead to performance deterioration.

However, RFI problem in HFPBR is mentioned a little in the open literature. Many temporal or time-frequency techniques are also discussed to remove RFI in HF active radar systems, but they are based on chirp signals or others [12–15]. In this paper, RFI in OFDM-based HFPBR is investigated. OFDM technique is a multicarrier modulation method with up to hundreds of subcarriers. For HFPBR systems with OFDM waveform, RFI will show different characteristics, because the radar waveform of PBR is new and different, which exploits OFDM technique and is originally designed for broadcasting. Thus the RFI model should be reanalyzed

during PBR signal processing and then a suitable method can be proposed. In this paper, a theoretical analysis of the range-domain correlation of RFI in OFDM-based HF radar is presented. The results provide a theoretical basis for RFI mitigation in the range domain. So a new RFI mitigation method is introduced. RFI is assumed stationary along each range swath and for a subset of slow-time data. First, after the direct-path wave is rejected, the echo signals at the far range bins seemed to only have the interference and noise, without the sea echo or target. Then the interference subspace is constructed using the echo signals at far range bins. Finally, RFI in the effective range bins is mitigated by projecting them onto the orthogonal subspace of the interference subspace, using the correlation among different range bins. The introduced method is easy to perform in practice and has been evaluated using the experimental data of DRM-based HFPBR.

This paper is organized as follows. Based on the signal processing diagram and waveform of PBR systems, the range-domain correlation of RFI in OFDM-based PBR is introduced in Section 2. The new RFI mitigation method is presented in Section 3. The analysis results on real data are given in Section 4 and conclusions are drawn in Section 5.

## 2. Range-Domain Correlation of RFI in OFDM-Based PBR

The RFI characteristics in radar signals are closely related to the waveform used by the radar system and the radar signal processing scheme. According to the signal processing scheme for HFPBR with OFDM waveform given in [11], the echo signals are filtered by the matching filter of the reference signal to acquire the echo signals at each range bin.

OFDM technique is exploited in DRM broadcast to cope with the complex environment in HF band. The transmitted baseband complex-envelope DRM signal during each symbol interval can be described by the following expression [16]:

$$s_r(t) = \sum_{k=K_{\min}}^{K_{\max}} C_k e^{j2\pi k \Delta f t} = \sum_{k=K_{\min}}^{K_{\max}} C_k e^{j2\pi f_k t}, \quad (1)$$

where  $k$  denotes the carrier number from  $K_{\min}$  to  $K_{\max}$ ;  $f_k = k\Delta f$  is the frequency for carrier  $k$ ;  $\Delta f$  is the carrier frequency interval; and  $C_k$  is the modulated complex cell value for carrier  $k$ .

In the receiver, baseband RFI is considered as a narrow band signal that can be represented as  $n(t)$ , which is the stationary baseband interfering signal with zero mean and bandwidth of  $B_n$ .

The range correlation is actually processing the received signal by a filter  $h(t)$  matched to the transmitted OFDM signal  $s_r(t)$ , so

$$h(t) = s_r^*(-t) = \sum_{k=K_{\min}}^{K_{\max}} C_k^* e^{j2\pi f_k t}, \quad (2)$$

where the superscript  $*$  denotes conjugate operation.

Thus the output of the range correlation of the RFI can be expressed as

$$\begin{aligned} y(\tau) &= n(t) \otimes h(t) = \int_{-\infty}^{\infty} \sum_{k=K_{\min}}^{K_{\max}} C_k^* e^{j2\pi f_k t} n(\tau - t) dt \\ &= \sum_{k=K_{\min}}^{K_{\max}} C_k^* \int_{-\infty}^{\infty} n(\tau - t) e^{j2\pi f_k t} dt \\ &= \sum_{k=K_{\min}}^{K_{\max}} C_k^* e^{j2\pi f_k \tau} N(f_k), \end{aligned} \quad (3)$$

where  $\otimes$  denotes the convolution operator and  $N(f_k) = \int_{-\infty}^{\infty} n(t) e^{-j2\pi f_k t} dt$ . It shows that the discrete samples of  $y(\tau)$  ( $y(\tau_n)$ ) actually are the Inverse Discrete Fourier Transform of  $C_k^* N(f_k)$ . Assuming  $c(t_n)$  and  $n(t_n)$  are the corresponding discrete time-domain expressions of  $C_k$  and  $N(f_k)$ , the discrete samples of  $y(\tau)$  can also be seen as  $c^*(-t_n) \otimes n(t_n)$ . It also shows that the interference after range correlation extends to all range bins.

The correlation function of the interference in the range domain can be written as

$$\begin{aligned} R_y(\tau, \tau - \alpha) &= E \{ y(\tau) y^*(\tau - \alpha) \} \\ &= E \left\{ \sum_{k=K_{\min}}^{K_{\max}} C_k^* N(f_k) e^{j2\pi f_k \tau} \cdot \sum_{l=K_{\min}}^{K_{\max}} C_l N^*(f_l) \right. \\ &\quad \cdot e^{-j2\pi f_l(\tau - \alpha)} \left. \right\} = E \left\{ \sum_k \sum_l C_k^* C_l N(f_k) N^*(f_l) \right. \\ &\quad \cdot e^{j2\pi f_k \tau} e^{-j2\pi f_l(\tau - \alpha)} \left. \right\} = \sum_k \sum_l E \{ C_k^* C_l N(f_k) \\ &\quad \cdot N^*(f_l) \} e^{j2\pi f_l \alpha} e^{j2\pi(f_k - f_l)\tau} = \sum_k |C_k N(f_k)|^2 e^{j2\pi f_k \alpha}, \end{aligned} \quad (4)$$

where  $E\{\cdot\}$  is the expectation operator. Obviously, the corresponding power spectrum is  $|C_k N(f_k)|^2$ . It shows that the correlation time of the incident interference is related to interference bandwidth  $B_n$  and the distribution of the modulated complex cell value  $C_k$ . Obviously, owing to the different waveform, the relevant result of RFI in OFDM-based passive radar is different from the one in chirp signal-based radar [15].

## 3. RFI Mitigation

The above analysis provides a theoretical basis for RFI mitigation in the range bin. As in DRM-based HFPBR, the mean of  $|C_k|$  is 1 and the variance is also very small. Then the correlation time of the incident interference can be approximated as  $\tau_n \approx 1/B_n$ . Thus as long as the interference bandwidth is relatively small, the interference will be correlated over a large number of range bins which is more than the effective detection range bins, and it ensures the efficiency

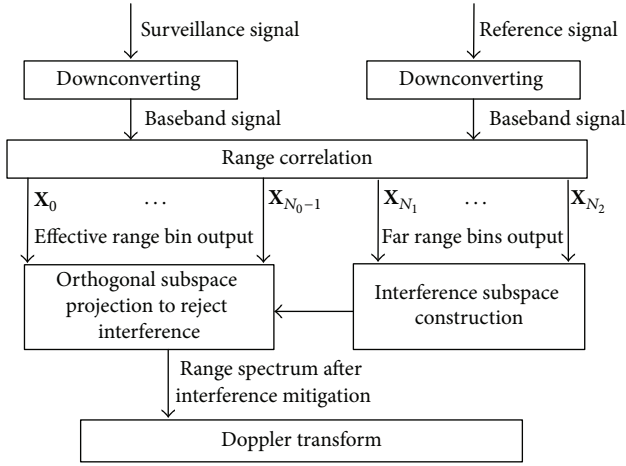


FIGURE 1: Flow chart of processing steps for RFI mitigation.

of the range-domain mitigation. An orthogonal projection filtering method for RFI mitigation in HFPBR is introduced in the following. The processing diagram is given in Figure 1.

In PBR, the strength of the direct-path wave can often be so strong to mask target echoes or RFI echoes. To uncover the RFI signal in the range domain, the direct-path wave should be rejected first. Then the surveillance signal and reference baseband signal are processed by range correlation to get different range bin samples.

Assume all the slow-time samples at  $n$ th range bin to be  $\mathbf{X}_n = [x_n(1), x_n(2), \dots, x_n(M)]^T$ , with  $M$  being the number of slow-time sample instants, where  $n$  is from 0 to maximum range bin number. It is known that the sea echoes and target signals attenuate greatly when the range increases, while the interference extends to all range bins with the power being independent of the range [13]. Assume the effective range bin is from 0 to  $N_0 - 1$ ; namely, the echoes of interest only occupy  $N_0$  range bins. There exists a reserved range segment where the range bin is far away from  $N_0$  but within the maximum range bin. And at the reserved range bins, it can be seen that there are only the interference and noise and no sea echo or target.

Assume the reserved range bins number is from  $N_1$  to  $N_2$ . The value of  $N_1$  and  $N_2$  should be larger than  $N_0$  and within the correlation range bin number. Then we can estimate the correlation matrix of the interference in the range domain as

$$\mathbf{R} = \frac{1}{N_2 - N_1} \sum_{n=N_1}^{N_2} \mathbf{X}_n \mathbf{X}_n^H, \quad (5)$$

where the superscript  $H$  denotes the conjugate transpose operator. Additionally, some advanced covariance matrix estimators could be used instead of the sample covariance to exploit information usually available at the receiver, such as the level of the white noise, the condition number of the matrix, and the effective rank, and achieve enhanced estimate [17–19]. Then the eigenvalue decomposition of the correlation matrix can be obtained as follows:

$$\mathbf{R} = \sum_{l=1}^{N_2 - N_1 + 1} \lambda_l \mathbf{U}_l \mathbf{U}_l^H, \quad (6)$$

where  $\lambda_l$  and  $\mathbf{U}_l$  are the eigenvalue and eigenvector. Without loss of generality, assume  $\lambda_1 > \lambda_2 > \dots > \lambda_{N_2 - N_1 + 1}$  and there is  $L$  relatively larger eigenvector which can be estimated by comparing the logarithms of  $\lambda_l$ . Owing to the fact that there are only the interference and noise at the reserved range bins, we can assume that  $L$  relatively larger eigenvector is the corresponding interference eigenvalues and  $\mathbf{U}_1, \mathbf{U}_2, \dots, \mathbf{U}_L$  are corresponding interference eigenvectors. Thus we can construct the interference subspace as  $\mathbf{V} = [\mathbf{U}_1, \mathbf{U}_2, \dots, \mathbf{U}_L]$ .

Then the signals at effective range bins can be projected onto the orthogonal subspace of  $\mathbf{V}$  to mitigate the interference. And the new signals at the effective range bins after interference mitigation  $\mathbf{X}_{n,\text{supp}}$  ( $n = 0, \dots, N_0 - 1$ ) are given by

$$\mathbf{X}_{n,\text{supp}} = (\mathbf{I} - \mathbf{V}\mathbf{V}^H) \mathbf{X}_n. \quad (7)$$

By the way, to mitigate the nonstationary RFI, short-time interference subspaces can be calculated in place of the global one, to do orthogonal projection filtering.

#### 4. Real Data Results

The introduced method was used in the practical DRM-based HFPBR experiment data. The experiment data was collected by the PBR system of Wuhan University, during August 2011. The radar system worked at a frequency of 8 MHz. The cooperative DRM broadcast transmitter was located in Qingdao City, along the east coast of Shandong Province, China. The receiving antenna array consisted of 16-element passive monopole helical antennas. The 16-element linear receiving array was placed along the coastline in Yantai City, Shandong Province, China, which was about 50 km far away from the transmitter whose peak power was about 500 W. So the system worked in a surface wave mode. After being processed by mixing, amplifying, and filtering in the analog frontend, the 16-element received signals were digitalized by the analog-to-digital converter. After digital downconversion, the data were processed on the platform and recorded in the disk array for offline analysis. In order to evaluate the performance of the introduced interference mitigation method, just one segment of the experimental data for this study is demonstrated.

The reference signal and the surveillance signal are obtained by making the receiving antenna array beam steer toward the transmitter and targets, respectively. And the sampling rate was 24 kHz and the coherent integration time is about 256 s, with  $M = 512$ . Figure 2 gives the RD map before direct-path wave rejection. The direct-path wave is too strong to show RFI or echoes of interest. Figure 3 shows the range spectrum after direct-path wave rejection by the minimum variance distortionless response (MVDR) adaptive beamformer [1], which shows that RFIs present as the bands arranged along the range bins in many time samples (about 58, from 165 to 175 and so on). Figure 4 shows the RD plot after direct-path wave rejection. As apparent, after the direct-path wave is rejected, the advancing and receding Bragg lines of sea echo can be seen. However, RFI covered a majority of the whole map, including the sea echoes' Bragg spectral

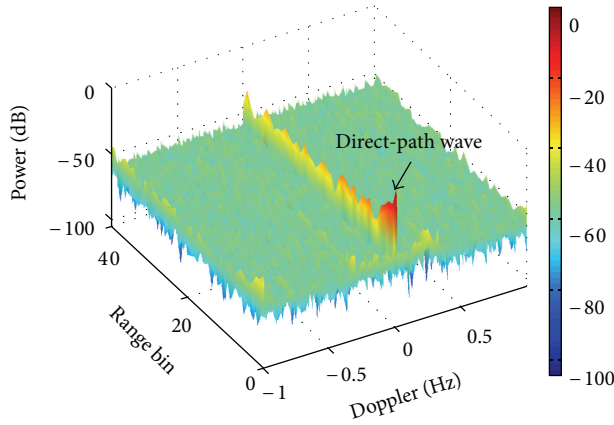


FIGURE 2: RD plot before direct-path wave rejection.

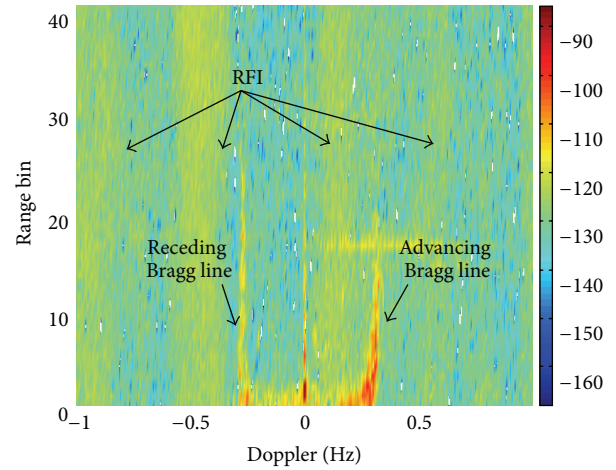


FIGURE 4: RD plot after direct-path wave rejection.

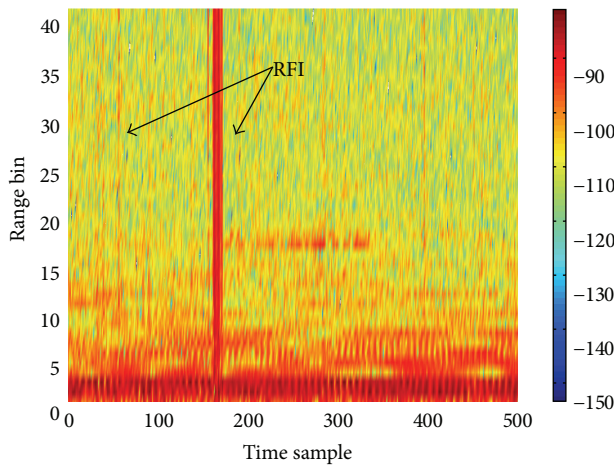


FIGURE 3: Range spectrum after direct-path wave rejection.

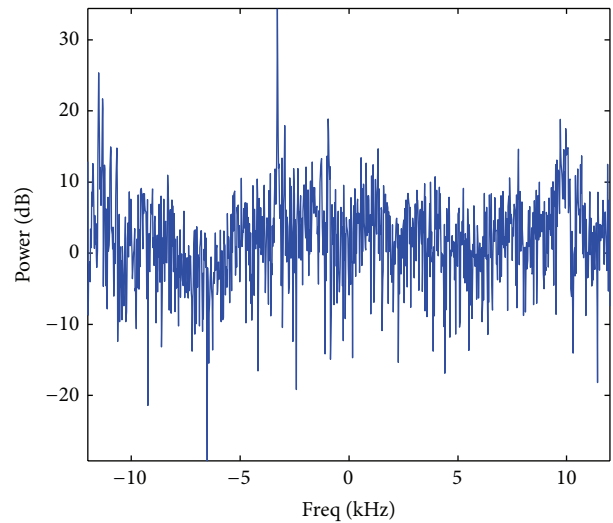


FIGURE 5: Frequency spectrum of time sample 58.

region. The orthogonal projection algorithm was used to mitigate the interference.

Figures 5 and 6 show the frequency spectra of time samples 58 and 167 appearing in RFI, respectively. We can see that the interference bandwidth is very small, not more than 300 Hz. It means that the correlation time is about  $1/300$  s, corresponding to 80 range bins. The effective detection bistatic range designed was 500 km corresponding to 40 range bins. So we select range bin indexed 50 to 80 as the reserved range bins. Figure 7 gives the eigenspectrum of the correlation function of signals at the reserved range bins. Here only the largest 32 eigenvalues were displayed.

Figure 8 gives the range spectrum after the effective range bins orthogonally projected onto the subspace. Here, the global interference subspace is calculated. It shows that the RFI is effectively mitigated by comparing Figures 8 and 3. Figure 9 presents the range bin 8 cuts with suspect vessel before and after RFI mitigation, from which we can also see that the spectral floor is assumed to be flat. The average interference suppression is about 5 dB. And Figure 10 presents the range bin 40 cuts before and after RFI mitigation, where the interference mitigation effect is more obvious.

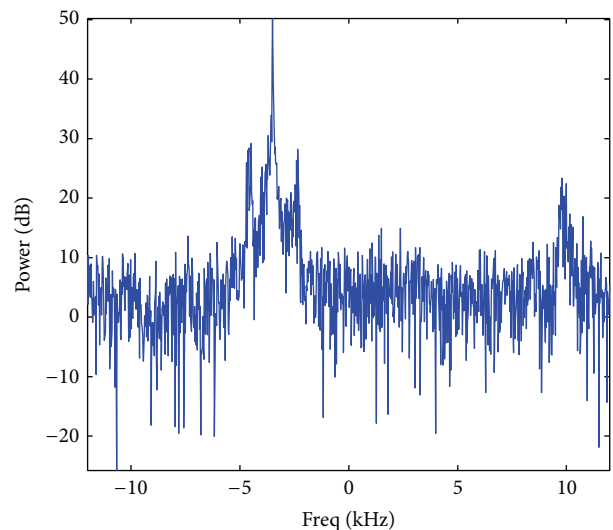


FIGURE 6: Frequency spectrum of time sample 167.

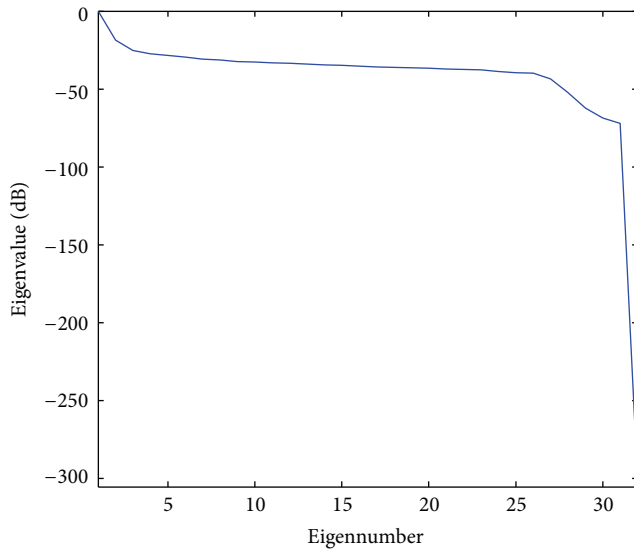


FIGURE 7: Eigenspectrum of the correlation function of signals at the reserved range bins.

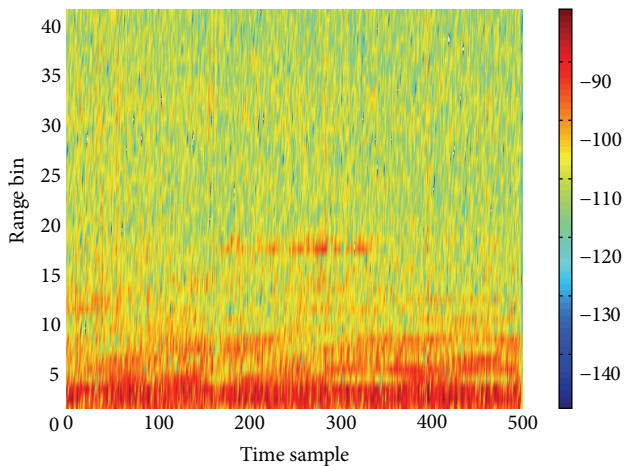
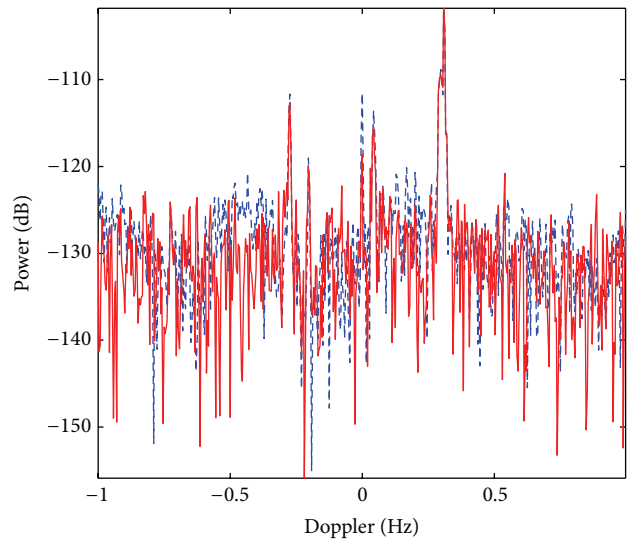


FIGURE 8: Range spectrum after clutter and RFI mitigation.

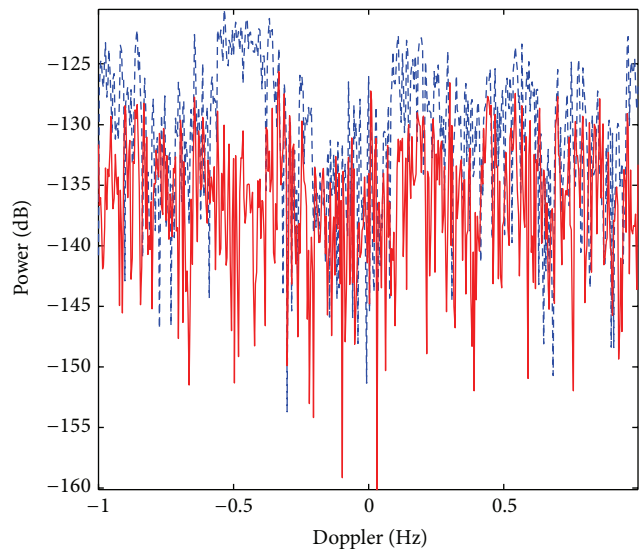
### 5. Conclusions

The RFI issues in HFPBR with OFDM waveform are investigated in this paper. For OFDM-based PBR, RFI in the surveillance channel is distributed regularly on the RD plot, which may mask targets as what the direct-path wave and multipath clutter do. A theoretical analysis of the range-domain correlation function of RFI in OFDM waveform passive radar is presented. The analysis provides theory basis for the proposal of a new RFI mitigation method in range domain. The method can mitigate RFI while almost bringing no loss to the echo signal of interest, which will greatly enhance the detection performance of HFPBR. The method is easy to perform. It can also be applied to other PBR with OFDM waveform. The experimental results have verified the theoretical analysis of the RFI and the validity of the introduced RFI mitigation method.



--- Before RFI mitigation  
— After RFI mitigation

FIGURE 9: Range bin 8 cuts before and after RFI mitigation by the introduced method.



--- Before RFI mitigation  
— After RFI mitigation

FIGURE 10: Range bin 40 cuts before and after RFI mitigation by the introduced method.

### Competing Interests

The authors declare that there is no conflict of interests regarding the publication of this paper.

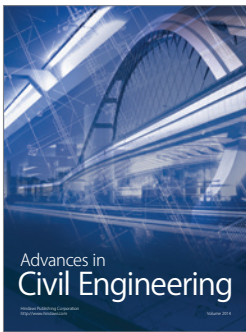
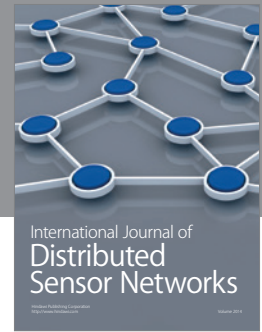
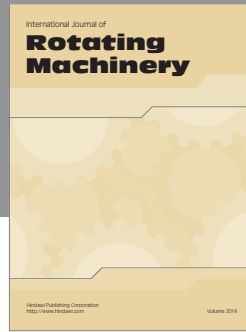
### Acknowledgments

Thanks are due to the Radio Detection and Research Center, School of Electronic Information, Wuhan University, for providing the experimental data used in this paper. This work

was supported in part by the National Science Fund Committee (NSFC) (no. 61461030), the National Science Fund of Jiangxi Province (20152ACB21008 and 20161BAB203079), the Young Scientists Training Program of Jiangxi Province (20142BCB23001), and the International Scientific Cooperation Projects of Jiangxi Province (20141BDH80001).

## References

- [1] Z. Zhao, X. Wan, D. Zhang, and F. Cheng, "An experimental study of HF passive bistatic radar via hybrid sky-surface wave mode," *IEEE Transactions on Antennas and Propagation*, vol. 61, no. 1, pp. 415–424, 2013.
- [2] N. Millet and M. Klein, "Passive radar air surveillance: last results with multi-receiver systems," in *Proceedings of the International Radar Symposium (IRS '11)*, pp. 281–285, Leipzig, Germany, September 2011.
- [3] J. Yi, X. Wan, H. Leung, and F. Cheng, "MIMO passive radar tracking under a single frequency network," *IEEE Journal of Selected Topics in Signal Processing*, vol. 9, no. 8, pp. 1661–1671, 2015.
- [4] S. Choi, D. Crouse, P. Willett, and S. Zhou, "Multistatic target tracking for passive radar in a DAB/DVB network: initiation," *IEEE Transactions on Aerospace and Electronic Systems*, vol. 51, no. 3, pp. 2460–2469, 2015.
- [5] Y. Feng, T. Shan, S. Liu, and R. Tao, "Interference suppression using joint spatio-temporal domain filtering in passive radar," in *Proceedings of the IEEE International Radar Conference (RadarCon '15)*, pp. 1156–1160, IEEE, Arlington, Va, USA, May 2015.
- [6] J. M. Thomas, C. J. Baker, and H. D. Griffiths, "DRM signals for HF passive bistatic radar," in *Proceedings of the 2007 IET International Conference on Radar Systems*, pp. 1–5, IET, Edinburgh, UK, 2007.
- [7] J. M. Thomas, C. J. Baker, and H. D. Griffiths, "Hf passive bistatic radar potential and applications for remote sensing," in *Proceedings of the New Trends for Environmental Monitoring Using Passive Systems (PASSIVE '08)*, pp. 1–5, Hyeres, France, October 2008.
- [8] C. J. Coleman, R. A. Watson, and H. Yardley, "A practical bistatic passive radar system for use with DAB and DRM illuminators," in *Proceedings of the IEEE Radar Conference (RADAR '08)*, pp. 1–6, IEEE, Rome, Italy, May 2008.
- [9] S. Sen and A. Nehorai, "Adaptive OFDM radar for target detection in multipath scenarios," *IEEE Transactions on Signal Processing*, vol. 59, no. 1, pp. 78–90, 2011.
- [10] R. Narasimhan, "Performance of diversity schemes for OFDM systems with frequency offset, phase noise and channel estimation errors," in *Proceedings of the IEEE International Conference on Communications (ICC '02)*, vol. 3, pp. 1551–1557, IEEE, New York, NY, USA, May 2002.
- [11] Z. Zhao, X. Wan, J. Yi, R. Xie, and Y. Wang, "Radio frequency interference mitigation in OFDM based passive bistatic radar," *AEU—International Journal of Electronics and Communications*, vol. 70, no. 1, pp. 70–76, 2016.
- [12] X. Luo, L. M. H. Ulander, J. Askne, G. Smith, and P.-O. Frörlind, "RFI suppression in ultra-wideband SAR systems using LMS filters in frequency domain," *Electronics Letters*, vol. 37, no. 4, pp. 241–243, 2001.
- [13] Y. H. Quan, M. D. Xing, L. Zhang, and Z. Bao, "Transient interference excision and spectrum reconstruction for OTHR," *Electronics Letters*, vol. 48, no. 1, pp. 42–44, 2012.
- [14] W. Wang and L. R. Wyatt, "Radio frequency interference cancellation for sea-state remote sensing by high-frequency radar," *IET Radar, Sonar and Navigation*, vol. 5, no. 4, pp. 405–415, 2011.
- [15] H. Zhou and B. Wen, "Radio frequency interference suppression in small-aperture high-frequency radars," *IEEE Geoscience and Remote Sensing Letters*, vol. 9, no. 4, pp. 788–792, 2012.
- [16] European Telecommunication Standards Institute (ETSI), *ETSI ES 201 980 V3.1.1-Digital Radio Mondiale (DRM); System Specification*, ETSI, 2009.
- [17] X. Guo, H. Sun, T. S. Yeo, and Y. Lu, "Lightning interference cancellation in high-frequency surface wave radar," in *Proceedings of the CIE International Conference on Radar (ICR '06)*, pp. 1–4, Shanghai, China, October 2006.
- [18] Y. I. Abramovich, N. K. Spencer, S. J. Anderson, and A. Y. Gorokhov, "Stochastic-constraints method in nonstationary hot-clutter cancellation. I. Fundamentals and supervised training applications," *IEEE Transactions on Aerospace and Electronic Systems*, vol. 34, no. 4, pp. 1271–1292, 1998.
- [19] M. W. Y. Poon, R. H. Khan, and S. Le-Ngoc, "A singular value decomposition (SVD) based method for suppressing ocean clutter in high frequency radar," *IEEE Transactions on Signal Processing*, vol. 41, no. 3, pp. 1421–1425, 1993.



**Hindawi**

Submit your manuscripts at  
<http://www.hindawi.com>

